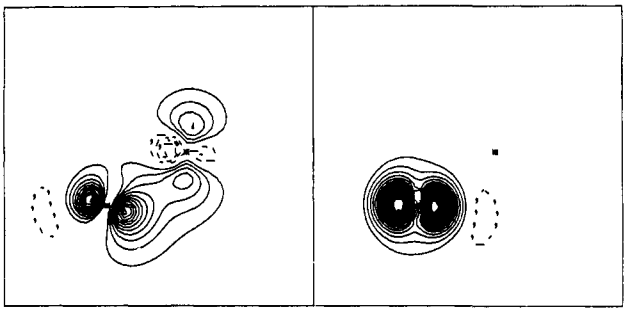

Figure 1. Contour plots of the two singlet-paired GVB-PP one-electron orbitals of a Zr–Pt bond. Solid lines represent positive contours while dashed lines represent negative contours. Contours are plotted every 0.04 au, ranging from −0.4 to +0.4 au. The asterisks represent nuclei, with one Pt atom at the lower left and the Zr atom to the right of center. The right panel shows an electron localized on Pt in an sd hybrid orbital, while the left panel shows an electron delocalized via an sd–sd interaction between Zr and Pt. This illustrates a superposition of sd–sd bonding and ionic bonding, since more than one electron is localized on Pt.

metallic dimer Pt_2 at the same level of theory. The states are split to a much greater degree than in the homometallic case, which we propose is due to the ionic nature of the bonding, as well as perhaps an increase in d–d interactions. These states all show a high degree of ionicity in the opposite direction from Engel–Brewer theory, with electrostatic interactions found to be at least as important as sp–sp or d–d metallic bonding. The electronic spectrum for $ZrPt_3$ at its bulk geometry shows a much lower density of states than in the homometallic Pt_3 cluster, indicating again that the bonding interactions are quite different. However, two states are very low-lying; the ^1A and ^3A states are separated by only 4 kcal/mol, making it difficult to predict, because of basis set biases, which state is the true ground state. The atomization energy of our predicted ground ^3A state is at least 101.1 kcal/mol, which suggests great thermal stability for the clusters as well as the bulk material. Significant electron transfer occurs from Zr to Pt_3 that is again contradictory to the assumptions in Engel–Brewer theory. Both localized electrostatic interactions as well as some sd–sd hybrid bonding between Zr and the three Pt atoms and the normal metallic sp–sp bonding within the Pt_3 moiety are found to be the important components in the formation of $ZrPt_3$.

In sum, these ab initio calculations suggest that bulk intermetallic compounds are more stable than their homometallic counterparts, but not because of pure d–d interactions and electron transfer from the late transition metal to the early transition metal as suggested previously.[1-4] Rather, the enhanced stability is due to electron transfer from the early transition metal to the late transition metal (which should have been expected based on their work functions) combined with sd–sd and sp–sp metallic interactions between the heterometallic and homometallic components of the alloy, respectively.

Acknowledgment. This work was supported by the Air Force Office of Scientific Research. E.A.C. acknowledges additional support from the National Science Foundation and the Camille and Henry Dreyfus Foundation via Presidential Young Investigator and Dreyfus Teacher-Scholar Awards, respectively.

Y-Conjugated Compounds: The Equilibrium Geometries and Electronic Structures of Guanidine, Guanidinium Cation, Urea, and 1,1-Diaminoethylene

Alberto Gobbi and Gernot Frenking*

Contribution from the Fachbereich Chemie, Philipps-Universität Marburg, Hans-Meerwein-Strasse, D-3550 Marburg, Germany. *Received July 24, 1992*

Abstract: Ab initio calculations at the MP2/6-31G(d) level of theory predict that the equilibrium geometries of the Y-conjugated compounds guanidine (**1**), guanidinium cation (**2**), urea (**5**), and 1,1-diaminoethylene (**6**) are nonplanar. **1**, **5**, and **6** have energy minimum structures with strongly pyramidal amino groups. The equilibrium geometry of the guanidinium cation **2b** has D_3 symmetry; the planar amino groups are rotated by ~15° out of the D_{3h} form **2a**. The planar structure **2a** becomes lower in energy than **2b** when corrections are made for zero-point vibrational energies. The observed planar geometries of guanidine and urea in the crystal are probably caused by hydrogen bonding. The resonance stabilization of the Y-conjugated structures is not very high, because the rotation of one amino group leaves a subunit which is isoelectronic to the allyl anion. Yet, resonance stabilization in the Y-conjugated forms is important, as it is revealed by the calculated rotational barriers for the NH_2 groups and the substantial lengthening of the C–NH_2 bonds upon rotation. The energy difference between 1,1-diaminoethylene (**6**) and 1,2-diaminoethylene (**7**) is mainly due to conjugative stabilization in **6**. The two isomers have nearly the same energy when one amino group in **6** is rotated. The calculated proton affinity of guanidine is only 237.7 kcal/mol. It is concluded that the very high basicity of **1** in solution is not caused by the resonance stabilization of **2**, but rather by strong hydrogen bonding of the guanidinium cation.

1. Introduction

The structure and properties of guanidine (**1**) and its associated acid, the guanidinium cation (**2**) (Figure 1), has attracted the interest of theoretical chemists for many decades.[1-9] Guanidine is one of the strongest organic bases (pK_a = 13.6)[10] known in chemistry, and guanidine and its derivatives are biologically and industrially important chemicals.[11] In fact, until the synthesis of the so-called "proton sponges",[12,13] **1** was considered *the* strongest organic base.

(1) Pauling, L. *The Nature of the Chemical Bond*, 3rd ed.; Cornell University Press: Ithaca, NY, 1960; p 286.
(2) Gund, P. *J. Chem. Educ.* **1972**, *49*, 100.
(3) Kollman, P.; McKelvey, J.; Gund, P. *J. Am. Chem. Soc.* **1975**, *97*, 1640.
(4) Capiiani, J. F.; Pedersen, L. *Chem. Phys. Lett.* **1978**, *54*, 547.
(5) Sapse, A. M.; Massa, L. J. *J. Org. Chem.* **1980**, *45*, 719.
(6) Ohwada, T.; Itai, A.; Ohta, T.; Shudo, K. *J. Am. Chem. Soc.* **1987**, *109*, 7036.
(7) Sreerama, N.; Vishveshwara, S. *J. Mol. Struct.* **1989**, *194*, 61.
(8) Williams, M. L.; Gready, J. E. *J. Comput. Chem.* **1989**, *10*, 35.
(9) Wiberg, K. B. *J. Am. Chem. Soc.* **1990**, *112*, 4177.
(10) Angyal, S. J.; Warburton, W. K. *J. Chem. Soc.* **1951**, 2492.
(11) *The Chemistry of Guanidine*; American Cyanamid Co.: Wayne, NJ, 1950.
(12) Alder, R. W.; Bryce, M. R.; Goode, N. C.; Miller, N.; Owen, J. *J. Chem. Soc., Perkin Trans. 1* **1981**, 2840.
(13) Staab, H. A.; Saupe, T. *Angew. Chem.* **1988**, *100*, 895; *Angew. Chem., Int. Ed. Engl.* **1988**, *27*, 865.

0002-7863/93/1515-2362$04.00/0

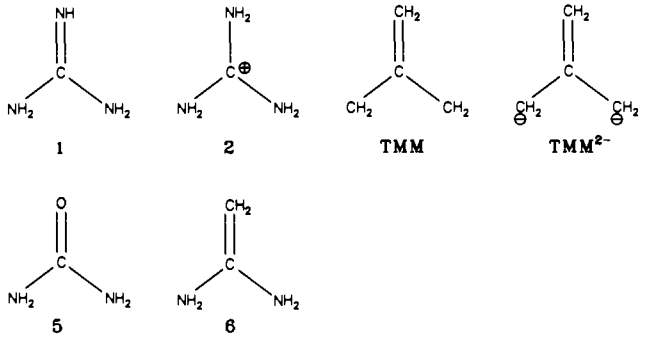

Figure 1. Schematic representation of the Y-conjugated molecules **1**, **2**, TMM, TMM^{2-}, **5**, and **6**.

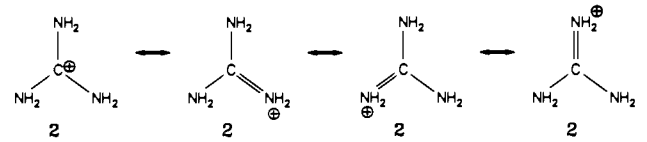

Figure 2. Resonance forms of **2**.

The standard textbook explanation for the exceptionally high basicity of **1** is given in terms of resonance theory.[1] Protonation of **1** is supposed to yield the highly symmetric cation **2**, which may be written using three equivalent resonance forms (Figure 2). Pauling[1] used valence bond theory to estimate that the cation was 6–8 kcal/mol more stable due to the gain in resonance energy. The high symmetry of the D_{3h} structure shown in Figure 2 suggests that **2** is strongly resonance stabilized. Guanidine-type resonance stabilization has been identified in many biologically important molecules,[8,9] since numerous biochemical compounds have substructures which are related to **1**. Isoelectronic to **1** is urea (**5**), which is another biologically important molecule. For example, enzymatic carboxyl-transfer reactions proceed via carboxylated biotin, a derivative of urea.[14] Several theoretical studies have been devoted to the electronic structure and properties of **5**.[8,15]

The Y-shaped conjugation in guanidine-type molecules is sometimes compared with the cyclic conjugation in annulenes. The high stability of the six π-electron system **2** is in sharp contrast to the predicted unstability of trimethylenemethane (TMM), which has four π-electrons.[16] The degenerate highest occupied molecular orbital (HOMO) of **2** is fully occupied, while TMM has only two electrons in the degenerate HOMO. When two electrons are added to TMM, the trimethylenemethane dianion (TMM^{2-}) is formed, which has six π-electrons. The analogy concerning symmetry, stability, and dependency upon the number of π-electrons let Gund[2] suggest that a new type of aromaticity, called "Y-aromaticity", is the reason for the high stability of **2** and related compounds. The theoretically predicted[2] stability of TMM^{2-} was later experimentally supported by the surprisingly facile lithiation of 2-methylpropene yielding TMM^{2-}.[17] Further experimental studies were reported as evidence for[18a] and against[18b] the stability of Y-aromatic species.

The suggestion of aromatic stability in Y-conjugated compounds such as **2** and TMM^{2-} was not undisputed. Klein[19] analyzed the structure of Y-conjugated compounds and concluded that favorable Coulombic interactions rather than Y-aromaticity are the main cause for their stability. This was supported by theoretical studies of delocalization in small ring dications and dianions by Schleyer,[20] who found that the preference for Y-delocalized isomers is caused by more favorable π charge distribution. For many years a controversial discussion about the reasons for the stability of Y-shaped compounds appeared in the literature.[9,18-23] A recent theoretical study of the importance of resonance interactions and Coulombic stabilization in Y-conjugated anions and cations by Wiberg[9] came to the conclusion that *neither* resonance stabilization *nor* favorable charge interactions stabilize **2** over **1** to a significant extent. It was speculated that the high basicity of **1** might rather be due to strong hydrogen bonding of **2** in polar solvents, and that guanidine is probably not a strong base in the gas phase.[9]

All theoretical studies devoted to the structures and stabilities of Y-conjugated molecules cited above[1-9,15,19,21,22] are based on the *assumption* that the investigated molecules are planar; i.e., the geometries of the molecules have always been optimized with the constraint of planarity.[24] Very recently, we published the first ab initio quantum mechanical study of the prototype of a Y-aromatic compound i.e., TMM^{2-}, which shows that the planar form of TMM^{2-} has four imaginary frequencies (MP2/6-31G(d)), and that the equilibrium structure has strongly pyramidalized methylene groups.[25,26] This poses the question about the equilibrium geometries of Y-shaped conjugated molecules and the importance of resonance effect in such compounds. This paper is an extension of our theoretical studies of Y-conjugated compounds. We wish to report the calculated equilibrium structures of guanidine (**1**), its conjugated acid **2**, urea (**5**), and 1,1-diaminoethylene (**6**). We will show by quantum mechanical ab initio calculations that *all investigated molecules* **1**, **2**, **5**, and **6** *are predicted to have nonplanar energy minimum structures*. Our report is the first theoretical study of guanidines, guanidinium cation, and urea in which the calculated equilibrium structures rather than planar forms are studied.[24,27] The electronic structure of the investigated molecules is analyzed by calculating the electron density distribution $\rho(\mathbf{r})$, the gradient vector field $\nabla\rho(\mathbf{r})$, and its associated Laplacian $\nabla^2\rho(\mathbf{r})$ as developed by Bader and co-workers.[28,29] Covalent bond orders P_{AB}, which are based on the topological theory of atoms in molecules, have been calculated by the procedure suggested by Cioslowski and Mixon.[30] Atomic charges were also computed using the natural bond orbital (NBO) method developed by Weinhold and co-workers.[31]

2. Theoretical Methods

The geometry optimization and energy calculations have been carried out using the program package Gaussian 90[32] and CADPAC.[33] We

(14) Lynen, F.; Knappe, J.; Lorch, E.; Jutting, G.; Ringlemann, E. *Angew. Chem.* **1959**, *71*, 481.
(15) (a) Thatcher, G. R. J.; Poirier, R.; Kluger, R. *J. Am. Chem. Soc.* **1986**, *108*, 2699. (b) Murray, J. S.; Politzer, P. *Chem. Phys. Lett.* **1988**, *152*, 364. (c) Koizumi, M.; Tachibana, A.; Yamabe, T. *J. Mol. Struct. (THEOCHEM)* **1988**, *164*, 37. (d) Del Bene, J. E. *Chem. Phys.* **1979**, *40*, 329.
(16) Weiss, F. *Q. Rev. Chem. Soc.* **1970**, *24*, 278.
(17) Klein, J.; Medlik-Balan, A. *J. Chem. Soc., Chem. Commun.* **1973**, 275.
(18) (a) Mills, N. S.; Shapiro, J.; Hollingsworth, M. *J. Am. Chem. Soc.* **1981**, *103*, 1264. (b) Mills, N. S. *J. Am. Chem. Soc.* **1982**, *104*, 5689.
(19) Klein, J. *Tetrahedron* **1988**, *44*, 503.
(20) Clark, T.; Wilhelm, D.; Schleyer, P. v. R. *Tetrahedron Lett.* **1982**, *23*, 3547.
(21) (a) Agranat, I.; Skancke, A. *J. Am. Chem. Soc.* **1985**, *107*, 867. (b) Agranat, I.; Radhakrishnan, T. P.; Herndon, W. C.; Skancke, A. *Chem. Phys. Lett.* **1991**, *181*, 117.
(22) (a) Inagaki, S.; Hirabayashi, Y. *Chem. Lett.* **1982**, 709. (b) Inagaki, S.; Kawata, H.; Hirabayasi, Y. *J. Org. Chem.* **1983**, *48*, 2928.
(23) Klein, J. *Tetrahedron* **1983**, *39*, 2733.
(24) After this study was completed, a theoretical study of urea and amide derivatives was published in which a nonplanar geometry for urea is predicted: Kontoyianni, M.; Bowen, J. P. *J. Comput. Chem.* **1992**, *13*, 657.
(25) Gobbi, A.; MacDougall, P. J.; Frenking, G. *Angew. Chem.* **1991**, *103*, 1023; *Angew. Chem., Int. Ed. Engl.* **1991**, *30*, 1001.
(26) A nonplanar geometry has been predicted for TMM^{2-} using semiempirical methods: Glukhotsev, M. N.; Simkin, B. Y. *Izv. Sev.-Kavk. Nauchn. Tsentra Vyssh. Shk. Estestv. Nauki* **1989**, *2*, 115; *Chem. Abstr.* **1990**, *113*, 5348f.
(27) 1,1-Diaminoethylene (**6**) has theoretically been studied before, and a nonplanar geometry was reported: Frenking, G. *J. Am. Chem. Soc.* **1991**, *113*, 2476.
(28) (a) Bader, R. F. W.; Tal, Y.; Anderson, S. G.; Nguyen-Dang, T. T. *Isr. J. Chem.* **1980**, *19*, 8. (b) Bader, R. F. W.; Nguyen-Dang, T. T.; Tal, Y. *Rep. Prog. Phys.* **1981**, *44*, 893. (c) Bader, R. F. W.; Nguyen-Dang, T. T. *Adv. Quantum Chem.* **1981**, *14*, 63.
(29) Bader, R. F. W. *Atoms in Molecules: A Quantum Theory*; Oxford University Press: Oxford, 1990.
(30) Cioslowski, J.; Mixon, S. T. *J. Am. Chem. Soc.* **1991**, *113*, 4142.
(31) Reed, A. E.; Curtiss, L. A.; Weinhold, F. *Chem. Rev.* **1988**, *88*, 899.
(32) Gaussian 90: Frisch, M. J.; Head-Gordon, M.; Trucks, G. W.; Foreman, J. B.; Schlegel, H. B.; Raghavachari, K.; Robb, M. A.; Binkley, J. S.; Gonzalez, C.; DeFrees, D. J.; Fox, D. J.; Whiteside, R. A.; Seeger, R.; Melius, C. F.; Baker, J.; Martin, R.; Kahn, L. R.; Stewart, J. J. P.; Topiol, S.; Pople, J. A. Gaussian Inc.: Pittsburgh, PA, 1990.

Table I. Calculated Total Energies E_{tot} (au), Relative Energies E_{rel} (kcal/mol), Number of Imaginary Frequencies i, and Zero-Point Energies **ZPE** (kcal/mol) for Different Conformations of **1** and **2**[a]

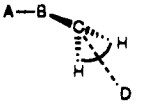

	1a	**1b**	**1c**	**2a**	**2b**	**2c**
symmetry	C_s	C_1	C_1	D_{3h}	D_3	C_s
E_{tot}	−204.7367 (−204.1135)	−204.7457 (−204.1199)	−204.7347 (−204.1083)	−205.1356 (−204.5215)	−205.1362	−205.117 (−204.5006)
E_{rel}	5.7 (4.0)	0.0 (0.0)	6.9 (7.3)	0.4 (0.0)	0.0	12.1 (13.1)
i	2 (2)	0 (0)	1 (1)	1 (0)	0	1 (1)
ZPE	42.9 (44.2)	44.8 (46.0)	44.1 (45.4)	51.0 (52.7)	51.6	51.8 (53.2)
C^1–N^2	1.382 (1.731)	1.400 (1.387)	1.378 (1.367)	1.334 (1.321)	1.334	1.399 (1.392)
C^1–N^3	1.374 (1.364)	1.396 (1.384)	1.442 (1.429)	1.334 (1.321)	1.334	1.324 (1.310)
C^1–N^4	1.288 (1.267)	1.284 (1.260)	1.284 (1.258)	1.334 (1.321)	1.334	1.316 (1.301)
N^2–C^1–N^3–N^4	180.0 (180.0)	179.2 (179.6)	176.8 (178.1)	180.0 (180.0)	180.0	180.0 (180.0)
H^9–N^4–C^1–N^2	0.0 (0.0)	8.3 (6.4)	2.0 (1.1)	180.0 (180.0)	165.1	180.0 (180.0)
C^1–N^2–D	180.0 (180.0)	134.5 (138.1)	148.9 (153.6)	180.0 (180.0)	180.0	132.9 (134.3)
N^3–C^1–N^2–D		103.0 (101.7)	87.3 (87.3)			0.0 (0.0)
C^1–N^3–D	180.0 (180.0)	130.7 (134.1)	118.1 (120.5)	180.0 (180.0)	180.0	180.0 (180.0)
N^2–C^1–N^3–D		109.0 (107.8)	179.0 (178.9)			
$p(C^1$–$N^2)$	0.929	0.954	0.979	1.039	1.040	0.978
$p(C^1$–$N^3)$	0.918	0.940	0.900	1.039	1.040	1.107
$p(C^1$–$N^4)$	1.420	1.442	1.458	1.039	1.040	1.119
$p(N^2$–$H^5)$	0.787	0.787	0.760	0.721	0.720	0.746
$p(N^2$–$H^6)$	0.780	0.800	0.792	0.721	0.720	0.746
$p(N^3$–$H^7)$	0.761	0.796	0.804	0.721	0.720	0.707
$p(N^3$–$H^8)$	0.790	0.779	0.808	0.721	0.720	0.718
$p(N^4$–$H^9)$	0.840	0.835	0.838	0.721	0.720	0.718
$p(N^4$–$H^{10})$				0.721	0.720	0.684

	1a		**1b**		**1c**		**2a**		**2b**		**2c**	
	NBO	Bader	NBO	Bader	NBO	Bader	NBO	Bader	NBO	Bader	NBO	Bader
$q(C^1)$	0.755	1.761	0.737	1.639	0.724	1.610	0.862	1.926	0.862	1.926	0.872	1.767
$q(N^2)$	−0.944	−1.299	−0.938	−1.195	−0.916	−1.260	−0.874	−1.305	−0.877	−1.308	−0.962	−1.112
$q(N^3)$	−0.933	−1.305	−0.932	−1.186	−0.958	−1.093	−0.874	−1.305	−0.877	−1.308	−0.852	−1.313
$q(N^4)$	−0.896	−1.240	−0.849	−1.251	−0.825	−1.247	−0.874	−1.305	−0.877	−1.308	−0.827	−1.308
$q(H^5)$	0.412	0.427	0.410	0.415	0.422	0.446	0.460	0.499	0.462	0.500	0.448	0.464
$q(H^6)$	0.419	0.436	0.403	0.404	0.402	0.415	0.460	0.499	0.462	0.500	0.448	0.464
$q(H^7)$	0.407	0.426	0.401	0.405	0.403	0.396	0.460	0.499	0.462	0.500	0.468	0.510
$q(H^8)$	0.433	0.457	0.418	0.426	0.400	0.391	0.460	0.499	0.462	0.500	0.462	0.498
$q(H^9)$	0.347	0.342	0.352	0.347	0.349	0.343	0.460	0.499	0.462	0.500	0.459	0.498
$q(H^{10})$							0.460	0.499	0.462	0.500	0.483	0.530
$q(N^2H_2)$	−0.113	−0.436	−0.125	−0.376	−0.092	−0.399	0.046	−0.307	0.047	−0.308	−0.066	−0.184
$q(N^3H_2)$	−0.093	−0.422	−0.113	−0.355	−0.155	−0.306	0.046	−0.307	0.047	−0.308	0.078	−0.305
$q(N^4H_x)$	−0.549	−0.898	−0.497	−0.904	−0.476	−0.904	0.046	−0.307	0.047	−0.308	0.094	−0.280

[a] Bond distances A–B (Å), bond angles A–B–C, and torsion angles A–B–C–D (deg). Calculated bond orders p(A–B) and partial charges q(A). All values at MP2/6-31G(d)//MP2/6-31G(d), values in parentheses at HF/6-31G(d)//HF/6-31G(d), point charges q(A) from NBO at HF/6-31G(d)//MP2/6-31G(d).

optimized the geometries and calculated the vibrational frequencies at the Hartree–Fock (HF) and MP2 (Møller–Plesset perturbation theory terminated at second order[34]) level of theory using the 6-31G(d) basis set.[35] These levels of theory are denoted HF/6-31G(d) and MP2/6-31G(d), respectively. The calculated zero-point vibrational energies (ZPE) at MP2/6-31G(d) are scaled by 0.92; the ZPE data calculated at HF/6-31G(d) are scaled by 0.89.[36] Unless otherwise noted, results are discussed at MP2/6-31G(d). Improved total energies were obtained using Møller–Plesset theory at third (MP3) and full fourth order (MP4) and the 6-311G(d,p) basis set[37] with the geometries optimized at MP2/6-31G(d).

For the calculation of the electron density distribution $\rho(r)$, the gradient vector field $\nabla\rho(r)$, and its associated Laplacian $\nabla^2\rho(r)$, the programs PROAIM, SADDLE, GRID, and GRDVEC were used.[38] The covalent bond orders P_{AB} have been computed using the program BONDER.[39] Atomic charges were also calculated with the NBO subroutine[40] implemented in Gaussian 90.

3. Results and Discussion

3.1. Guanidinium (1) and Guanidinium Cation (2). The theoretically predicted structures for **1** and **2** are shown in Figure 3. The calculated bond lengths and angles and the results of the population analyses are listed in Table I. The planar (C_s) form of guanidine **1a** has two imaginary frequencies and, therefore, is a second-order saddle point. The equilibrium structure **1b**, which is 5.7 kcal/mol (6.7 kcal/mol at MP4/6-311G(d,p), Table III) lower in energy than **1a**, has strongly pyramidal NH_2 groups (bending angles 130.7° and 134.5°). The energy difference between **1a** and **1b** is reduced to 3.8 kcal/mol (4.8 kcal/mol at MP4/6-311G(d,p), Table III), when corrections are made for ZPE

(33) Cadpac 4.0: Amos, R. D.; Rice, J. E. *CADPAC: The Cambridge Analytical Derivatives Package*; Cambridge University Press: Cambridge, England, 1987.
(34) (a) Møller, C.; Plesset, M. S. *Phys. Rev.* **1934**, *46*, 618. (b) Binkley, J. S.; Pople, J. A. *Int. J. Quantum. Chem* **1975**, *9S*, 229.
(35) Hehre, W. J.; Ditchfield, R.; Pople, J. A. *J. Chem. Phys.* **1972**, *56*, 2257.
(36) Houi, R. F.; Levi, B. A.; Hehre, W. J. *J. Comput. Chem.* **1982**, *3*, 234.
(37) Krishnan, R.; Binkley, J. S.; Seeger, R.; Pople, J. A. *J. Chem. Phys.* **1980**, *72*, 650.
(38) Biegler-König, F. W.; Bader, R. F. W.; Ting-Hua, T. *J. Comput. Chem.* **1982**, *3*, 317.
(39) BONDER: Cioslowski, J.; Florida State Universiiy, 1991.
(40) NBO 3.0: Glendening, E. D.; Reed, A. E.; Carpenter, J. E.; Weinhold, F. Departmeni of Chemistry, Universiiy of Wisconsin: Madison.

Table II. Results of the Topological Analysis for the Wave Function of **1b**, **1c**, **2b**, and **2c** Calculated at MP2/6-31G(d)//MP2/6-31G(d)[a]

	1b				**1c**				**2b**				**2c**			
	ρ_b	H_b	r_b	ϵ_b	ρ_b	H_b	r_b	ϵ_b	ρ_b	H_b	r_b	ϵ_b	ρ_b	H_b	r_b	ϵ_b
C^1–N^2	0.305	−0.439	0.376	0.111	0.313	−0.494	0.355	0.140	0.346	−0.581	0.354	0.199	0.318	−0.378	0.433	0.069
C^1–N^3	0.311	−0.446	0.381	0.128	0.290	−0.341	0.416	0.014	0.346	−0.581	0.354	0.199	0.348	−0.595	0.344	0.202
C^1–N^4	0.386	−0.677	0.355	0.345	0.386	−0.680	0.352	0.360	0.346	−0.581	0.354	0.199	0.355	−0.614	0.343	0.231
N^2–H^5	0.323	−0.450	0.754	0.041	0.325	−0.455	0.761	0.043	0.320	−0.446	0.770	0.035	0.316	−0.440	0.762	0.038
N^2–H^6	0.325	−0.453	0.752	0.040	0.325	−0.454	0.754	0.042	0.320	−0.446	0.770	0.035	0.316	−0.440	0.762	0.038
N^3–H^7	0.323	−0.450	0.752	0.040	0.321	−0.447	0.750	0.033	0.320	−0.446	0.770	0.035	0.320	−0.447	0.773	0.032
N^3–H^8	0.324	−0.452	0.757	0.037	0.321	−0.446	0.749	0.034	0.320	−0.446	0.770	0.035	0.318	−0.443	0.770	0.029
N^4–H^9	0.319	−0.439	0.739	0.003	0.317	−0.436	0.738	0.006	0.320	−0.446	0.770	0.035	0.319	−0.445	0.770	0.027
N^4–H^{10}									0.320	−0.446	0.770	0.035	0.317	−0.430	0.777	0.030

[a] Electron density at the bond critical point ρ_b ($1/B^3$), energy density at the bond critical point H_b (au/B^3), location of the bond critical point r_b given by the distance ratio A–r_b/A–B, ellipticity at the bond critical point ϵ_b.

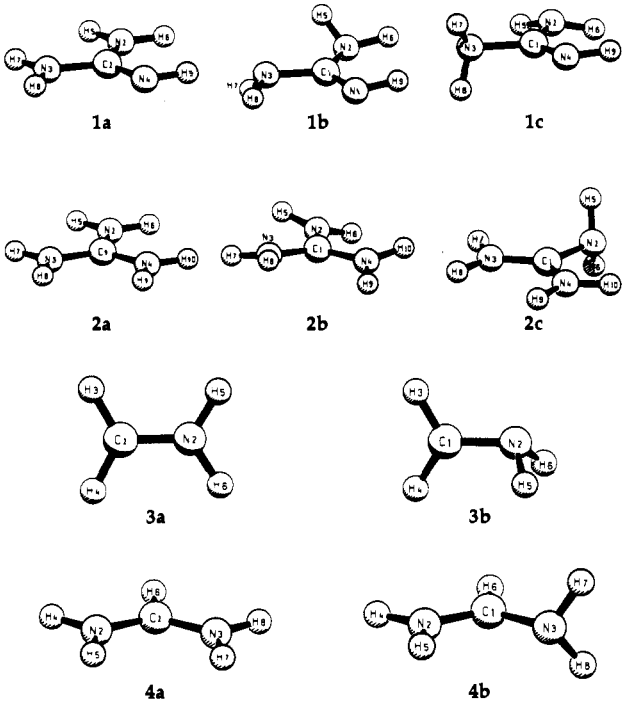

Figure 3. Optimized geometries for different conformations of compounds **1**, **2**, **3**, and **4**.

contributions (Table I). There is no experimentally determined geometry for guanidine available. The infrared spectrum of guanidine in the solid state was interpreted in favor of a planar form.[41] However, the very broad nature of the NH stretching modes showed clearly the presence of strong hydrogen bonding.[41]

The C–NH bond in **1b** is clearly shorter (1.284 Å) than the C–NH_2 bonds (1.396 Å and 1.400 Å). The covalent bond order for the C–NH bond is 1.442, while the C–NH_2 bonds are essentially covalent single bonds (P_{AB} = 0.954 and 0.940). For comparison, the C–N triple bond in HCN has a P_{AB} value of 2.24 (HF/6-31G(d)).[30] For **1b**, both methods of population analysis indicate a strong positive charge at the carbon atom and negatively charged NH_2 and NH groups. The absolute values predicted by the Bader method are significantly larger than calculated by the NBO procedure, but the trends are the same. The NH group carries more negative charge than the NH_2 groups (Table I).

We optimized the transition state for rotation about the C–NH_2 bond in **1c**. The activation barrier is calculated as 6.9 kcal/mol (Table I). This is reduced to 6.2 kcal/mol with inclusion of ZPE contributions. Calculations at higher levels give nearly the same results (Table III). Figure 4 shows the Laplacian distribution for **1b**. The results of the topological analysis of the wave function are listed in Table II. Inspection of the diagrams shown in Figure 4 indicates that the C–N bonds are strongly polarized toward nitrogen. This becomes obvious by the location of the bond critical points r_b. They are much closer to the carbon atom and assign a larger area of the C–N bond to nitrogen. The degree of polarization for a bond A–B may be given by the ratio of the distances A–r_b/A–B. A value of <0.5 indicates that r_b is closer to A than to B. The results listed in Table II show that the C–NH bond is more polarized toward nitrogen than the C–NH_2 bonds. The differences between the C–NH bond and the C–NH_2 bonds are exhibited in Figure 4, b and c. The Laplacian distribution shows that the C–NH bond is characterized by a π-bond which is polarized toward nitrogen, whereas the C–NH_2 bonds exhibits an area of electron concentration at N which can be identified as a lone-pair electron. The energy density at the bond critical point H_b, which may be taken as a measure for the covalency of the bond,[42] is much more negative for the C–NH bond (−0.677) than for the C–NH_2 bonds (−0.439, −0.446; Table II). The calculated ellipticity at the bond critical point ϵ_b, which is a measure for the π-bond character,[43] indicates that the C–NH bond has a much higher π-character (ϵ_b = 0.345) than the C–NH_2 bonds (ϵ_b = 0.111, 0.128). A pure σ-bond would have ϵ_b = 0.0, and ethylene has ϵ_b = 0.399 (MP2/6-31G(d)//MP2/6-31G(d)). Thus, the C–NH bond in **1b** has nearly the same π-character as the C–C bond in ethylene. Upon rotation, the C–NH_2 bond in **1c** becomes nearly a σ-bond (ϵ_b = 0.014), while the π-character of the other C–N bond increases (Table II).

The planar form of the guanidinium cation **2a** is predicted at HF/6-31G(d) as a minimum on the potential energy surface. However, at MP2/6-31G(d) **2a** is calculated with one imaginary frequency. The energy minimum structure **2b** at MP2/6-31G(d) has D_3 symmetry; the planar NH_2 groups are rotated around the C–NH_2 bonds by 15° (Table I). The X-ray structure analysis of the hexamethyl-substituted derivative of **2**, $C(NMe_3)_3^+$, shows planar amino groups rotated by 30° – 34° around the C–NMe_2 bonds.[44] Also, **2b** is 0.4 kcal/mol lower in energy than **2a**. We have calculated the energy difference between **2a** and **2b** at higher levels of theory (Table III). The difference remains small, but **2b** is always lower in energy than **2a**. With inclusion of ZPE corrections, the planar form **2a** is more stable than **2b** by 0.2 kcal/mol. The C–NH_2 bonds of **2a** and **2b** are calculated with the same bond length (1.334 Å), which are ~0.065 Å shorter than the C–NH_2 bonds in **1b** (Table I). The theoretically predicted C–NH_2 interatomic distances for the guanidinium ion are in excellent agreement with experimental values derived from vibrational spectra and X-ray structure analysis (1.33–1.35 Å).[45] Experimental studies[45,46] suggest that **2** has D_{3h} symmetry, but

(41) Jones, W. J. *Trans. Faraday Soc.* **1959**, *55*, 524.

(42) (a) Cremer, D.; Kraka, E. *Angew. Chem.* **1984**, *96*, 612; *Angew. Chem., Int. Ed. Engl.* **1984**, *23*, 627. (b) Cremer, D.; Kraka, E. *Croat. Chem. Acta* **1985**, *57*, 1265.

(43) The ellipticity (anisotropy) at the bond critical point is given by $\epsilon_b = (\lambda^1/\lambda^2) - 1$, where λ^1 and λ^2 are the principal curvatures perpendicular to the bond path: Bader, R. F. W.; Slee, T. S.; Cremer, D.; Kraka, E. *J. Am. Chem. Soc.* **1983**, *105*, 5061.

(44) (a) Bingel, C. Doctoral Thesis, Philipps-Universität Marburg, 1992. (b) Boese, R.; Bläser, D.; Petz, W. *Z. Naturforsch.* **1988**, *43b*, 945.

(45) (a) Angell, C. L.; Sheppard, N.; Yamaguchi, A.; Shimanouchi, T.; Miyazawa, T.; Mizushima, S. *Trans. Faraday Soc.* **1957**, *53*, 589. (b) Drenth, J.; Drenth, W.; Vos, A.; Wiebenga, E. H.; *Acta Cryst.* **1953**, *6*, 424. (c) Otvos, J. W.; Edsall, J. T. *J. Chem. Phys.* **1939**, *7*, 632. (d) Kellner, L. *Proc. R. Soc. London* **1941**, *A177*, 456.

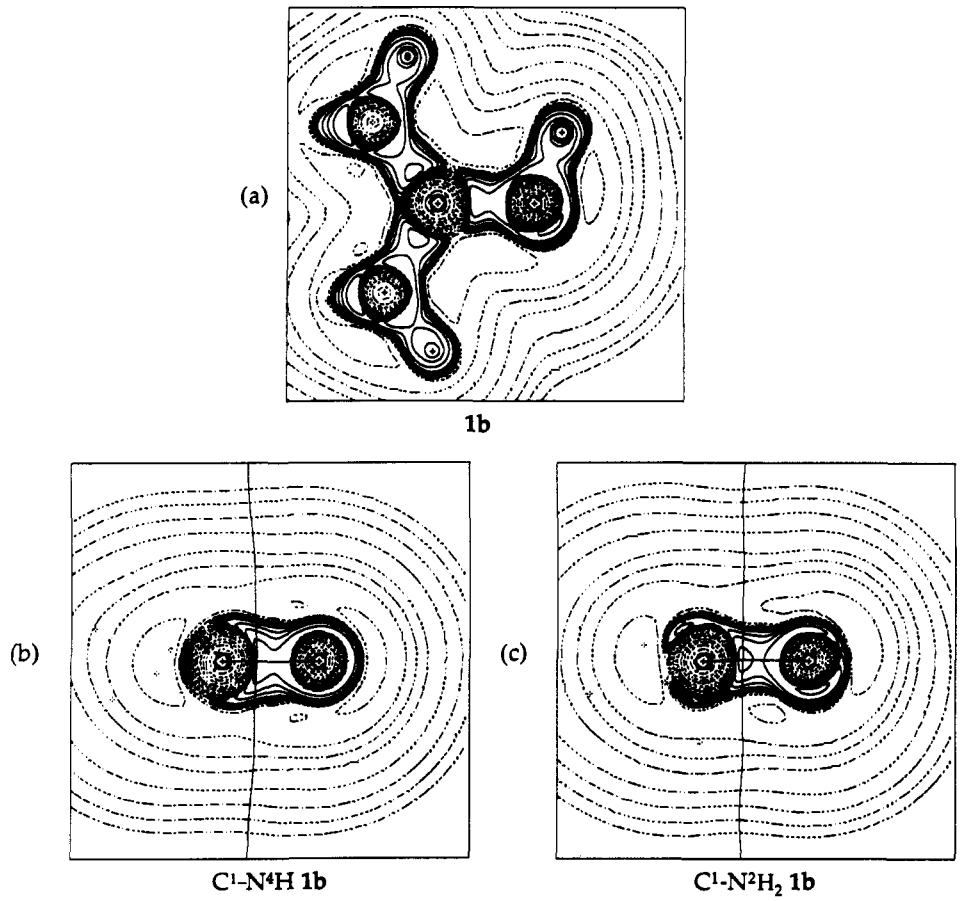

Figure 4. Contour line diagrams of the calculated Laplace distribution $-\nabla^2\rho(r)$ for the equilibrium geometry of guanidine (**1b**): (a) in the plane of the carbon and nitrogen atoms (nitrogen atoms of NH_2 groups slightly below the plane); (b) in the plane containing the C^1–N^4H bond perpendicular to the C^1–N^4–H^9 plane; (c) in the plane containing the C^1–N^2H_2 bond, bisecting the N^2H_2 group. In (b) and (c) the carbon atom is at the left side; the nitrogen atom is at the right side. Dashed contour lines are in regions of charge depletion and solid lines in regions of charge concentration. The solid line connecting the atomic nuclei is the bond path. The solid line crossing the bond path at the bond critical point indicates the zero-flux surface in the plane.

Table III. Calculated Total Energies E_{tot} (au) and Relative Energies E_{rel} (kcal/mol) for Structures **1** to **7**

	MP2/ 6-311G(d,p)//		MP3/6-311G(d,p)// MP2/6-31G(d)		MP4/ 6-311G(d,p)//	
	E_{tot}	E_{rel}	E_{tot}	E_{rel}	E_{tot}	E_{rel}
1a	−204.8493	6.0	−204.8673	6.0	−204.9021	6.7
1b	−204.8589	0.0	−204.8769	0.0	−204.9128	0.0
1c	−204.8481	6.8	−204.8663	6.7	−204.9025	6.5
2a	−205.2496	0.3	−205.2725	0.1	−205.3038	0.4
2b	−205.2501	0.0	−205.2727	0.0	−205.3044	0.0
2c	−205.2315	11.7	−205.2544	11.5	−205.2869	11.0
3a	−94.7216	0.0	−94.7400	0.0	−94.7563	0.0
3b	−94.6013	75.5	−94.6230	73.4	−94.6230	83.6
4a	−149.9990	0.0	−150.0186	0.0	−150.0432	0.0
4b	−149.9596	24.7	−149.9810	23.6	−150.0053	23.8
5a	−224.7366	3.1	−224.7450	3.1	−224.7843	3.5
5b	−224.7415	0.0	−224.7499	0.0	−224.7899	0.0
5c	−224.7288	8.0	−224.7371	8.0	−224.7778	7.6
6a	−188.7906	9.0	−188.8180	9.0	−188.8488	9.8
6b	−188.8050	0.0	−188.8323	0.0	−188.8644	0.0
6c	−188.7957	5.8	−188.8234	5.6	−188.8557	5.5
7a	−188.7781	16.9	−188.8055	16.8	−188.8370	17.2
7b	−188.7941	6.8	−188.8220	6.5	−188.8543	6.3

the clear observation of IR forbidden fundamentals in the vibrational spectrum of **2** in the solid state was interpreted as a sign for distortion of the site-symmetry in the crystal.[46]

While the energy difference between **2a** and **2b** is quantitatively not important, it is qualitatively significant. If conjugation would be as strong and important for the stability of **2**, why is it that the 1,5-repulsion between the adjacent hydrogen atoms, which is weak due to the large H–H distances, is sufficient to rotate the NH_2 groups by 15°?

We calculated the barrier for rotation of one NH_2 group in **2**. The optimized transition state structure **2c** has two planar NH_2 groups, while the rotating amino group is strongly pyramidalized (bending angle 132.9°, Table I). The rotational barrier is predicted to be 12.3 kcal/mol (MP2/6-31G(d) + ZPE), which is in excellent agreement with the experimental value of 13 kcal/mol obtained through NMR techniques.[47] The activation barrier is 11.2 kcal/mol at MP4/6-311G(d,p) + ZPE (Table III). What is the reason for this barrier? Wiberg[9] suggested that "most of the barrier probably resulted from the decrease in the volume over which the charge is distributed when one NH_2 group was rotated". Table I shows the changes in the geometry and electronic structure between **2b** and **2c**. The C–NH_2 bond of the rotating NH_2 group becomes clearly longer (1.399 Å), and the C–NH_2 bonds of the planar NH_2 groups become slightly shorter (1.316 Å and 1.324 Å) in **2c** than the C–NH_2 bonds in **2b** (1.334 Å). The significant lengthening of the C–NH_2 bond upon rotation of the NH_2 group is clear evidence for the conjugation of the nitrogen lone-pair electrons in **2b**. In **2c**, one nitrogen lone pair is orthogonal to the π-orbitals of the 1,3-diazaallyl moiety. The latter is isoelectronic with the allyl anion, and the electronic structure of **2** may be rationalized as 2-substituted allyl anion. The molecular orbital diagram for the π-orbitals of a 2-substituted allyl anion is shown in Figure 5a.

(46) Mecke, R.; Kuizelnigg, W. *Spectrochim. Acta* **1960**, *16*, 1225.

(47) Bally, T.; Diehl, P.; Haselbach, E.; Tracey, A. *Helv. Chim. Acta* **1975**, *58*, 2398.

Scheme I. Calculated Reaction Energies at MP2/6-31G(d)//MP2/6-31G(d)[a]

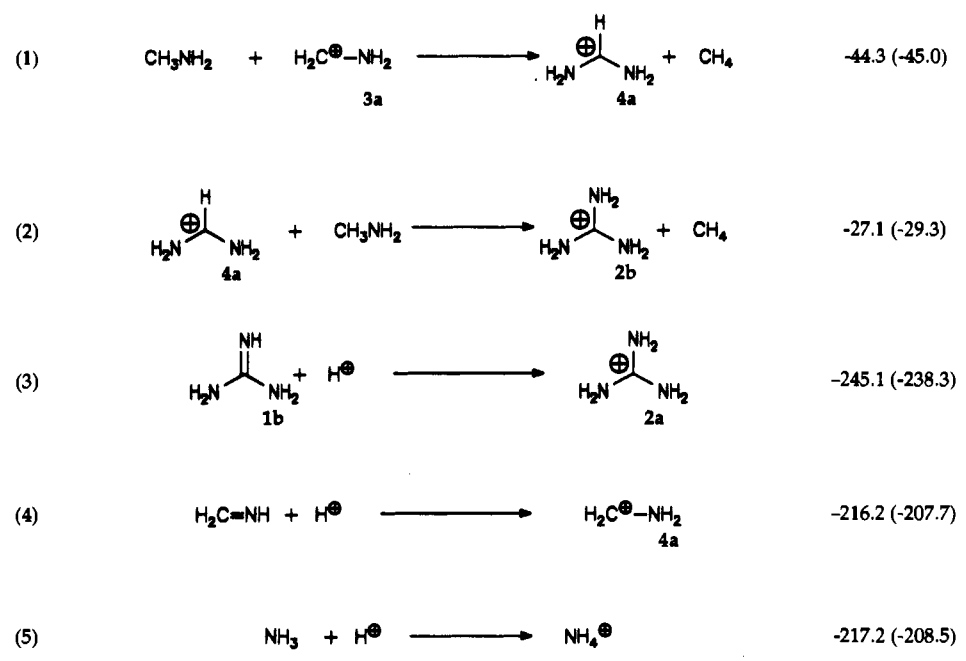

[a] Values in parentheses include the ZPE corrections.

Table IV. Calculated Data for Structures **3a**, **3b**, **4a**, and **4b**[a]

	3a	**3b**	**4a**	**4b**
symmetry	C_{2v}	C_s	C_{2v}	C_s
E_{tot}	−94.6676 (−94.3832)	−94.5441 (−94.2761)	−149.9156 (−149.4638)	−149.8746 (−149.4248)
E_{rel}	0.0 (0.0)	77.5 (67.2)	0.0 (0.0)	25.7 (24.5)
i	0 (0)	1 (1)	0 (0)	1 (1)
ZPE	31.9 (32.7)	28.4 (29.3)	42.5 (43.5)	41.6 (42.7)
C^1–N^2	1.282 (1.263)	1.354 (1.357)	1.313 (1.299)	1.287 (1.268)
C^1–N^3			1.313 (1.299)	1.389 (1.383)
C^1–N^2–D	180.0 (180.0)	119.3 (124.2)	180.0 (180.0)	180.0 (180.0)
C^1N^3–D			180.0 (180.0)	127.4 (129.1)
$p(C^1$–$N^2)$	1.438	1.260	1.181	1.319
$p(C^1$–$N^3)$			1.181	1.052

	3a		**3b**		**4a**		**4b**	
	NBO	Bader	NBO	Bader	NBO	Bader	NBO	Bader
$q(C^1)$	0.231	0.751	0.598	0.601	0.526	1.384	0.581	1.182
$q(N^2)$	−0.691	−1.264	−1.010	−1.092	−0.814	−1.314	−0.702	−1.277
$q(N^3)$					−0.814	−1.314	−0.967	−1.103
$q(H^3)$	0.254	0.220	0.236	0.252				
$q(H^4)$	0.254	0.220	0.214	0.224	0.469	0.520	0.473	0.530
$q(H^5)$	0.475	0.536	0.481	0.508	0.453	0.505	0.478	0.542
$q(H^6)$	0.475	0.536	0.481	0.508	0.258	0.194	0.237	0.189
$q(H^7)$					0.453	0.505	0.450	0.471
$q(CH_2)$	0.739	1.191	1.048	1.077				
$q(N^2H_2)$	0.259	−0.192	−0.048	−0.076	0.108	−0.289	0.249	−0.205
$q(N^3H_2)$					0.108	−0.289	−0.067	−0.161

[a] For details see Table I.

The π-orbital of the substituent cannot interact with the HOMO of the allyl anion because of symmetry. The interaction of the substituent π-orbital with the next highest occupied MO (NHOMO) and the LUMO gives three orbitals: a lower lying NHOMO, a nonbonding occupied orbital which gives a degenerate HOMO in the resulting Y system, and a higher lying antibonding LUMO. In terms of Hückel-type resonance energy,[48] the increase is only 0.318 β (Figure 5). This is because the rotation of one NH_2 group in **2** still leaves an allyl system intact. The conjugation in the allyl system of **2c** is larger than in the allyl moiety of **2b**, because there are only three p(π) orbitals in the NHOMO of **2c**, but there are four p(π) orbitals in the NHOMO of **2b**. This explains why the C–NH_2 bonds of the planar amino groups in **2c** are shorter than in **2b**. The loss of conjugative stabilization in the Y-conjugated system upon rotation of one amino group in **2c** is partially compensated by the increase in the resonance energy of the azaallyl system. Thus, the additional gain in conjugative stabilization in **2b** over **2c** is rather small.

Structure **2** may be considered as a triply substituted carbenium ion. In order to quantify the stabilization gained by substitution of hydrogen by the amino groups, we calculated the stabilization energies of the isodesmic reactions[49] 1 and 2 shown in Scheme I. The calculated energies[50] and results of the population analyses

(48) Heilbronner, E.; Bock, H. *Das HMO-Modell und seine Anwendung*; Verlag Chemie: Weinheim, 1968.

(49) Hehre, W. J.; Pople, J. A. *J. Am. Chem. Soc.* **1970**, *92*, 2191.

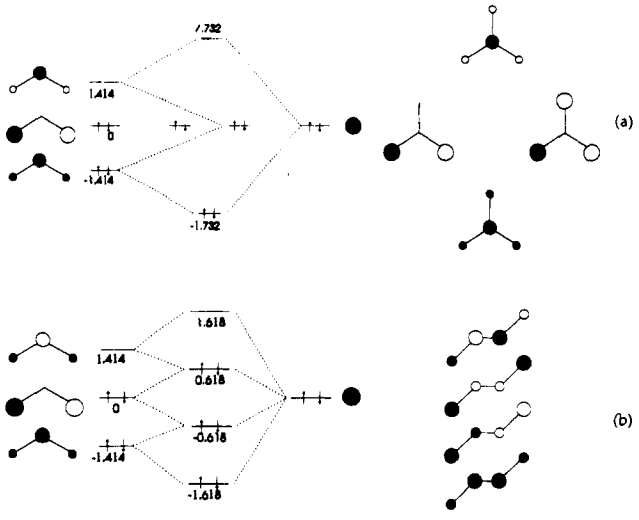

Figure 5. Qualitative molecular orbital diagram for the interaction of a, occupied p(π) orbital with allyl anion (a) in the 2-position; (b) in the 1-position. The resulting orbitals are shown at the right.

for **3a**, **3b**, **4a**, and **4b** are listed in Table IV.

Consider first the amino-substituted methyl cation $CH_2NH_2^+$ (**3**). Substitution of one methylene hydrogen by an amino group yields the diaminomethyl cation **4**, which is stabilized relative to **3** by 44.3 kcal/mol (Scheme I). The third amino group in **2b** gives an additional stabilization by only 27.1 kcal/mol relative to **4** (reaction 2, Scheme I). In reaction 1, the 2π molecule **3** is changed into the 4π molecule **4**, while in reaction 2 the 4π molecule **4** is changed into the 6π system **2**. The calculated energies for the isodesmic reactions 1 and 2 are clear evidence that there is *no* special stabilization in Y-conjugated systems which can be compared to the $4n + 2$ π-electron stabilization exhibited by cyclic annulenes. There is no aromaticity in Y-conjugated systems!

Conjugation between the nitrogen lone-pair electrons and the formally empty carbon p(π) orbital is much stronger in **3** and **4** than in **2**. The energy minimum structures **3a** and **4a** are both planar (Table IV, Figure 3). The activation barriers for rotation of one NH_2 group in **3** and **4** are significantly higher (**3**, 77.5 kcal/mol; **4**, 25.7 kcal/mol, Table IV) than in **2** (12.1 kcal/mol, Table I). Nearly the same results are predicted at higher levels of theory (Table III). There is a strong donation of the nitrogen lone-pair electrons into the formally empty p(π) orbital at CH_2 in **3a**, which becomes evident by the much longer C-NH_2 distance in **3b** (1.354 Å) than in **3a** (1.282 Å, Table IV). The resonance stabilization by a second amino group in **4a** is weaker, because the p(π) orbital at carbon atom is partly filled by the donation of the first amino group. Rotation of one amino group of **4a** yields one short C-NH_2 bond in **4b** with nearly the same bond length (1.287 Å) as in **3a** (1.282 Å). The third amino group in **2b** stabilizes the cation even less. The rotation of one NH_2 group in **2c** leaves an azaallyl system with C-NH_2 bond distances which are similar (1.316 Å, 1.324 Å) to **4a** (1.313 Å, Tables I and IV).

What importance does the charge distribution have for the stabilization of **2** relative to **1**? Table I shows the charge distribution calculated by the NBO[31] and Bader[29] methods for the equilibrium geometries **1b** and **2b**. Both methods predict that the protonation of **1** gives a higher positive charge at the carbon atom and larger negative charges at the nitrogen atoms. The two methods assign positive partial charges of the same magnitude to the hydrogen atoms; they differ in the absolute values for the charges at N and C. What about the change in the Coulombic interactions when one amino group is rotated from **2b** to **2c**? The negative charge concentration at nitrogen atom of the rotating amino group should become larger, because electronic charge cannot be donated from the N lone-pair electrons into the carbon p(π) orbital in **2c**. This should *increase* the charge attraction between C and the rotating NH_2 group.

Table I shows the charge distribution for **2b** and **2c**. As expected, the NBO method predicts that the rotating NH_2 group in **2c** carries a higher negative charge and the carbon atom a more positive charge than in **2b**. But the Bader method predicts the opposite trend! How can this result be explained? In order to analyze the electronic structure of guanidinium cation in more detail, the one-electron density distribution $\rho(\mathbf{r})$, its associated gradient field $\nabla\rho(\mathbf{r})$, and Laplacian $\nabla^2\rho(\mathbf{r})$ were calculated. Figure 6 shows the contour lines of $\nabla^2\rho(\mathbf{r})$ and the zero-flux surfaces separating the NH_2 groups from the carbon atom and the C-NH_2 bond paths for **2b** and **2c**. Table II shows the results of the topological analysis of the electronic wave function.

Inspection of the diagram shown in Figure 6, a and b, clearly shows that the π-electron distribution of the C-NH_2 bonds in **2b** is shifted toward the nitrogen atom. At nitrogen, there is concentration ($\nabla^2\rho(\mathbf{r}) < 0$, solid lines) in the π-electron area, while there is depletion at the carbon atom. The Laplacian distribution for **2c** (Figure 6c) shows a nonbonded charge concentration at the nitrogen atom of the rotating amino group, which is interpreted as a lone pair. The shift in the charge distribution is also revealed by the location of the C-NH_2 bond critical points r_b. This is shown in Figure 6, d and e, and in Table II. In **2b**, the bond critical points, which are the crossing points of the zero-flux surfaces and the bond paths, are closer to C than to N. The topology of the C-NH_2 bond indicates that a larger part of the electronic charge belongs to nitrogen than to carbon atom (Figure 6d). In **2b**, the ratio C-r_b/C-N is 0.354 (Table II). The location of the C-NH_2 bond critical point is significantly shifted toward nitrogen when the NH_2 group is rotated. The ratio C-r_b/C-N^2 in **2c** is 0.433 (Table II, Figure 6e). Thus, the topological analysis of the change in the electronic charge between **2b** and **2c** indicates that the shift in π-density toward nitrogen upon rotation of the amino group induces a concomitant countermigration of the σ-density to the carbon atom. This σ/π equilibrium has been observed and rationalized before.[25,51]

The C-NH_2 bond in **2b** may be compared with the C-NH and C-NH_2 bonds in **1b** using the results of the topological analysis shown in Table II and Figures 4 and 6. For the location of the bond critical point r_b of the C-NH_2 bond in **2b**, nearly the same ratio C-r_b/C-N (0.354) is calculated for the C-NH bond in **1b** (0.355, Table II). However, the Laplacian distributions shown in Figures 4b and 6b indicate that the π-bond in **2b** is more polarized toward nitrogen atom. The calculated ϵ_b values show that the C-NH_2 bonds in **2b** have a higher π-character (0.199) than the C-NH_2 bonds in **1b** (0.111, 0.128; Table II). As with guanidine (**1**), the π-character of the C-N bond is greatly reduced upon rotation around the C-N bond; ϵ_b is only 0.069 in **2c** (Table II). The increase in the interatomic distance as well as the much lower ϵ_b values for the rotating C-NH_2 bond in **1c** and **2c** are a strong indication that **1b** and **2b** are stabilized by π-conjugation.

The alteration in the topology of the electronic charge between **2b** and **2c** explains the counterintuitive change in the charge distribution calculated by the Bader method. If the NBO charges are taken into consideration, the rotation of the NH_2 group should give *stronger* charge attraction between carbon atom and the rotating amino group in **2c** than in **2b**, while the charges calculated by the topological analysis give the opposite result.[52] This illuminates the dilemma of trying to quantify the model of charge interactions for the explanation of chemical phenomena.[19,23] Any population analysis is based on an arbitrary decision for assigning charges to atoms. In the present case, the significantly longer C-NH_2 bond of the rotating amino group in **2c** can best be explained by the lack of conjugation of the nitrogen lone-pair electrons with the 2-azaally system. Thus, the additional stabi-

(50) The total energies in au (ZPE values in kcal/mol) at MP2/6-31G(d)//MP2/6-31G(d) for the molecules shown in Scheme I which are not given in the tables are: **3a**, -94.6676 (34.7); **4a**, -149.9156 (46.2); CH_4, -40.3370 (29.1); CH_3NH_2, -95.5144 (41.4); CH_2NH, -94.3231 (25.5); NH_3, -56.3574 (22.2); NH_4^+, -56.7036 (31.7).

(51) Slee, T. S.; MacDougall, P. J. *Can. J. Chem.* **1988**, *66*, 2961.

(52) Here we take only the charges, not the distances between them as measure for the charge interaction.

Table V. Calculated Data for Structures **5a**, **5b**, and **5c**[a]

	5a	**5b**	**5c**
symmetry	C_{2v}	C_2	C_1
E_{tot}	−224.6179 (−223.9822)	−224.6221 (−223.9847)	−224.6092 (−223.9704)
E_{rel}	2.6 (1.7)	0.0 (0.0)	8.1 (9.0)
i	2 (2)	0 (0)	1 (1)
ZPE	36.2 (37.1)	37.6 (38.6)	36.9 (38.0)
C^1–O^2	1.227 (1.202)	1.225 (1.197)	1.224 (1.196)
C^1–N^3	1.374 (1.360)	1.389 (1.373)	1.355 (1.344)
C^1–N^4	1.374 (1.360)	1.389 (1.373)	1.451 (1.433)
C^1–N^3–D	180.0 (180.0)	137.9 (142.7)	180.0 (180.0)
C^1–N^4–D	180.0 (180.0)	137.9 (142.7)	116.7 (119.4)
O^2–C^1–N^3–N^4	180.0 (180.0)	180.0 (180.0)	180.0 (180.0)
O^2–C^1–N^4–D		77.5 (78.7)	0.0 (0.0)
$p(C^1$–$O^2)$	1.134	1.174	1.206
$p(C^1$–$N^3)$	0.913	0.936	0.969
$p(C^1$–$N^4)$	0.913	0.936	0.886

	5a		**5b**		**5c**	
	NBO	Bader	NBO	Bader	NBO	Bader
$q(C^1)$	0.988	2.086	0.988	1.971	0.981	1.927
$q(O^2)$	−0.768	−1.253	−0.746	−1.236	−0.728	−1.228
$q(N^3)$	−0.942	−1.303	−0.943	−1.222	−0.915	−1.313
$q(N^4)$	−0.942	−1.303	−0.943	−1.222	−0.990	−1.089
$q(H^5)$	0.427	0.457	0.419	0.435	0.421	0.450
$q(H^6)$	0.404	0.428	0.402	0.417	0.426	0.464
$q(H^7)$	0.404	0.428	0.402	0.417	0.402	0.392
$q(N^3H_2)$	−0.111	−0.418	−0.122	−0.370	−0.068	−0.399
$q(N^4H_2)$	−0.111	−0.418	−0.122	−0.370	−0.186	−0.305

[a] For details see Table I.

Table VI. Calculated Data for Structures **6a**, **6b**, and **6d**

	6a	**6b**	**6c**
symmetry	C_{2v}	C_2	C_1
E_{tot}	−188.6791 (−188.0867)	−188.6937 (−188.0983)	−188.6839 (−188.0882)
E_{rel}	9.2 (7.3)	0.0 (0.0)	6.1 (6.3)
i	3 (3)	0 (0)	1 (1)
ZPE	48.8 (49.9)	51.0 (52.2)	50.3 (51.6)
C^1–C^2	1.350 (1.337)	1.344 (1.328)	1.344 (1.326)
C^1–N^3	1.384 (1.375)	1.405 (1.397)	1.395 (1.386)
C^1–N^4	1.384 (1.375)	1.405 (1.397)	1.442 (1.432)
C^1–C^2–D	180.0 (180.0)	180.0 (180.0)	178.8 (178.8)
C^1–N^3–D	180.0 (180.0)	130.6 (133.0)	137.1 (140.1)
C^1–N^4–D	180.0 (180.0)	130.6 (133.0)	123.6 (126.1)
C^2–C^1–N^3–N^4	180.0 (180.0)	180.0 (180.0)	176.2 (177.6)
N^3–C^1–C^2–H^5	0.0 (0.0)	9.4 (7.3)	1.9 (1.2)
N^3–C^1–C^2–D			111.6 (109.9)
C^2–C^1–N^3–D		69.1 (70.2)	94.1 (92.3)
C^2–C^1–N^4–D		69.1 (70.2)	8.0 (6.7)
$p(C^1$–$C^2)$	1.685	1.736	1.761
$p(C^1$–$N^3)$	0.949	0.968	0.987
$p(C^1$–$N^4)$	0.949	0.968	0.934
$p(C^2$–$H^5)$	0.973	0.969	0.970
$p(C^2$–$H^6)$	0.973	0.969	0.968
$p(N^3$–$H^7)$	0.781	0.806	0.806
$p(N^3$–$H^8)$	0.793	0.799	0.782
$p(N^4$–$H^9)$	0.793	0.799	0.814
$p(N^4$–$H^{10})$	0.781	0.806	0.819

	6a		**6b**		**6c**	
	NBO	Bader	NBO	Bader	NBO	Bader
$q(C^1)$	0.485	0.932	0.448	0.785	0.425	0.757
$q(C^2)$	−0.698	−0.141	−0.627	−0.135	−0.591	−0.137
$q(N^3)$	−0.913	−1.294	−0.909	−1.166	−0.896	−1.196
$q(N^4)$	−0.913	−1.294	−0.909	−1.166	−0.941	−1.104
$q(H^5)$	0.204	0.038	0.208	0.046	0.206	0.047
$q(H^6)$	0.204	0.038	0.208	0.046	0.209	0.050
$q(H^7)$	0.414	0.436	0.395	0.395	0.393	0.397
$q(H^8)$	0.401	0.423	0.396	0.400	0.405	0.420
$q(H^9)$	0.401	0.436	0.396	0.400	0.396	0.389
$q(H^{10})$	0.414	0.423	0.395	0.395	0.392	0.382
$q(C^2H_2)$	−0.290	−0.065	−0.211	−0.043	−0.176	−0.040
$q(N^3H_2)$	−0.098	−0.435	−0.118	−0.371	−0.098	−0.379
$q(N^4H_2)$	−0.098	−0.435	−0.118	−0.371	−0.153	−0.333

[a] For details see Table I.

Table VII. Calculated Data for Structures **7a** and **7b**[a]

	7a	**7b**
symmetry	C_{2v}	C_1
E_{tot}	−188.6677 (−188.0718)	−188.6833 (−188.0869)
E_{rel}	16.3 (16.7)	6.5 (7.2)
i	3 (3)	0 (0.0)
ZPE	48.8 (50.0)	51.1 (52.4)
N^1–C^2	1.395 (1.392)	1.399 (1.390)
C^2–C^3	1.345 (1.323)	1.343 (1.322)
C^3–N^4	1.395 (1.392)	1.434 (1.430)
N^1–C^2–C^3–N^4	180.0 (180.0)	−3.5 (−3.1)
C^2–N^1–D	180.0 (180.0)	130.3 (133.9)
C^3–N^4–D	180.0 (180.0)	126.9 (127.9)
C^3–C^2–N^1–D		81.0 (78.7)
C^2–C^3–N^4–D		150.8 (165.8)
$p(N^1$–$C^2)$	0.992	1.056[b] 1.020[c]
$p(C^2$–$C^3)$	1.764	1.749[b] 1.755[c]
$p(C^3$–$N^4)$	0.992	0.996[b] 0.978[c]
$p(C^2$–$H^5)$	0.933	0.925[b] 0.938[c]
$p(C^3$–$H^6)$	0.933	0.943[b] 0.958[c]
$p(N^1$–$H^7)$	0.796	0.810[b] 0.810[c]
$p(N^1$–$H^8)$	0.802	0.759[b] 0.754[c]
$p(N^4$–$H^9)$	0.796	0.823[b] 0.818[c]
$p(N^4$–$H^{10})$	0.802	0.817[b] 0.822[c]
$p(N^4$–$H^8)$	0.056	0.044[b] 0.096[c]

	7a		**7b**	
	NBO	Bader	NBO	Bader
$q(N^1)$	−0.930	−1.289	−0.901	−1.186
$q(C^2)$	−0.076	0.399	0.032	0.373
$q(C^3)$	−0.076	0.399	−0.144	0.288
$q(N^4)$	−0.930	−1.289	−0.938	−1.136
$q(H^5)$	0.209	0.054	0.205	0.056
$q(H^6)$	0.209	0.054	0.190	0.042
$q(H^7)$	0.404	0.426	0.387	0.387
$q(H^8)$	0.392	0.411	0.408	0.422
$q(H^9)$	0.404	0.426	0.380	0.375
$q(H^{10})$	0.392	0.411	0.382	0.377
$q(N^1H_2)$	−0.134	−0.452	−0.106	−0.377
$q(N^4H_x)$	−0.134	−0.452	−0.176	−0.384

[a] For details see Table I. Relative energies are given in relation to **6b** (Table VI). [b] Bad error value in Bonder. [c] Because of the very flat electron density, these values may not be accurate.

lization of **2** over **4** is mainly due to resonance effects, although the stabilization is much less than what might have been expected from the high basicity of **2**. This explains why the equilibrium geometry of **2b** has slightly rotated NH_2 groups.

Then what is the reason for the exceptionally high basicity of guanidine? The energy difference of **1** and **2** calculated at their equilibrium structures **1b** and **2b** gives a protonation energy of 238.3 kcal/mol (MP2/6-31G(d) + ZPE, Scheme I). At the same level of theory, the proton affinity of CH_2NH is predicted as 207.7 kcal/mol. This is nearly the same value as calculated for NH_3 (208.5 kcal/mol, Scheme I). The experimental value for the proton affinity of NH_3 is 205.0 kcal/mol.[53] Thus, **1** is calculated with a gas-phase proton affinity which is about 30 kcal/mol higher than ammonia. This makes the intrinsic basicity of guanidine as comparable to tri-*n*-butylamine (*n*-Bu_3N), which has an experimentally derived gas-phase proton affinity of 234.8 kcal/mol, 29.8 kcal/mol higher than NH_3.[53] But the pK_a value of *n*-Bu_3N is only 10.83,[54] three orders of magnitude lower than the pK_a of guanidine (13.6).[10] It follows that the high basicity of guanidine is *not* a property which can be explained by the molecular structure of isolated **1** and **2**. Guanidine is a molecule which has an unusually high proton affinity for an imine, but the very high basicity of **1** in solution is partly caused by other reasons, perhaps by strong hydrogen bonding of the cation **2** as suggested by Wiberg.[9]

3.2. Urea (5) and 1,1-Diaminoethylene (6). The optimized structures of urea (**5**), 1,1-diaminoethylene (**6**), and *cis*-1,2-di-

(53) Aue, D. H.; Bowers, M. T. In *Gas Phase Ion Chemistry*; Bowers, M. T., Ed.; Academic Press: New York, 1979; Vol. 2, p 16.

(54) Damsgaard-Sørensen, P.; Unmack, A. *Z. Phys. Chem.* (*A*) **1932**, *160*, 45.

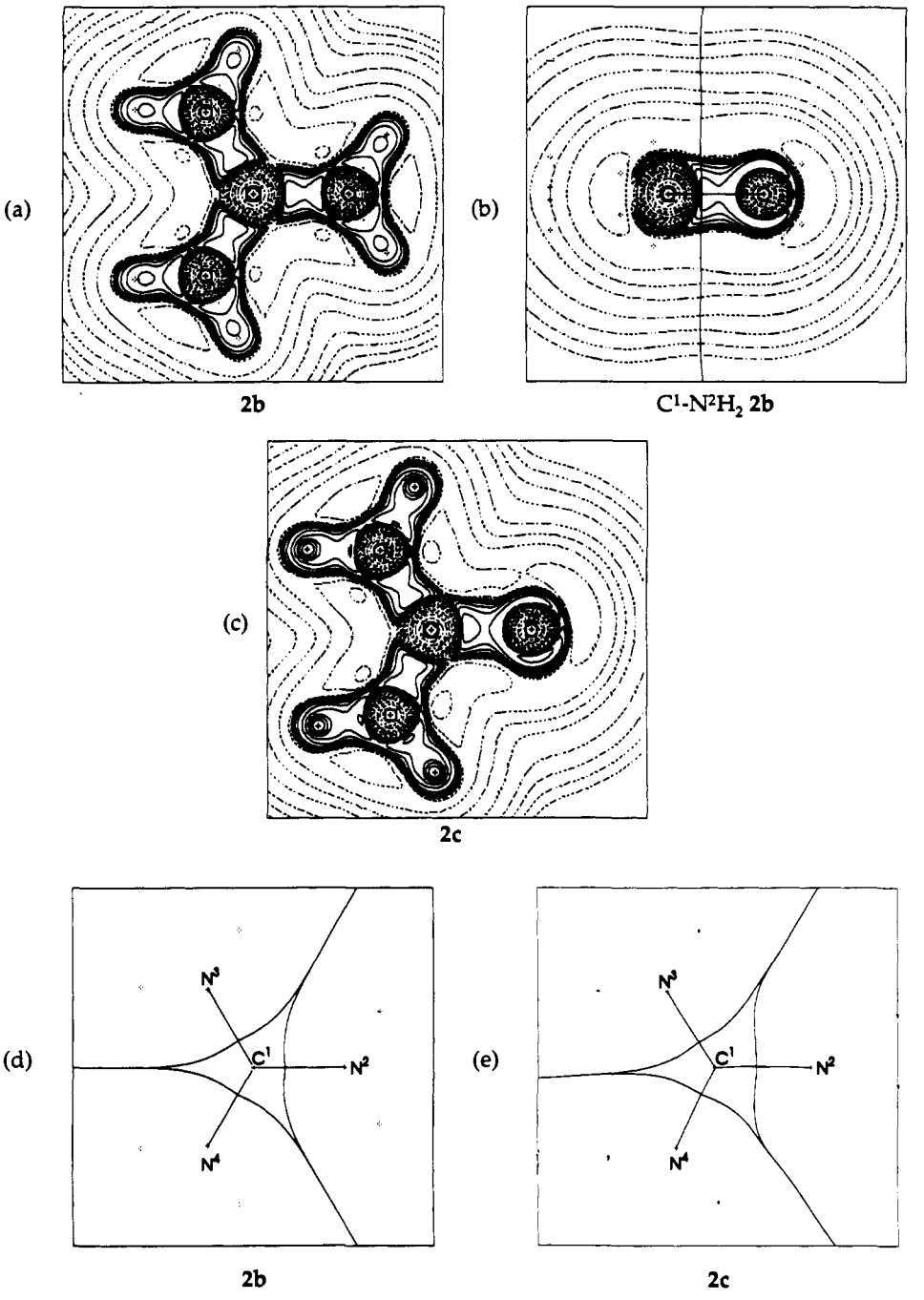

Figure 6. Contour line diagrams of the calculated Laplace distribution $-\nabla^2\rho(r)$ for the equilibrium geometry of: (a) guanidinium cation **2b** in the plane of the C and N atoms; (b) **2b** in the plane containing the $C^1-N^2H_2$ bond perpendicular to the NH_2 plane; (c) **2c** in the plane of the C and N atoms. Zero-flux surfaces separating the C and N atoms and $C-NH_2$ bond paths for (d) **2b** in the plane of C and N atoms; (e) **2c** in the plane of the C and N atoms. For details see Figure 4.

aminoethylene (**7**) in different conformations are shown in Figure 7; the calculated bond lengths and angles and the results of the population analyses are shown in Tables V–VII.

Optimization of the planar (C_{2v}) form of urea (**5a**) gives a structure which had two imaginary frequencies, both at the HF/6-31G(d) and MP2/6-31G(d) level of theory. The equilibrium geometry of urea (**5b**) has C_2 symmetry with strongly pyramidalized amino groups (bending angle 137.9°, Table V).[24] The energy difference between **5a** and **5b** is 1.7 kcal/mol at HF/6-31G(d) and 2.6 kcal/mol at MP2/6-31G(d). The energy difference is slightly higher at MP4/6-311G(d,p) (3.5 kcal/mol, Table III). However, ZPE contributions reduce the energy difference by 1.5 kcal/mol (HF/6-31G(d)) and 1.4 kcal/mol (MP2/6-31G(d), Table V). This makes the barrier for inversion of the amino groups very small. Experimental results obtained from neutron diffraction measurements and X-ray analysis indicate that the equilibrium geometry of urea in the solid state is planar.[55] However, the structure of urea is strongly affected by the crystal package, particularly by intermolecular hydrogen bonding between oxygen and amino hydrogen atoms.[55e] This accounts for the fact that the barrier of rotation around the $C-NH_2$ bond in the solid state was estimated from normal coordinate analysis as 25.9 kcal/mol[56a] and 30.1 kcal/mol.[56b] The theoretically predicted

(55) (a) Andrew, M. R.; Hyndman, D. Hyndman, D. *Proc. Phys. Soc. A* **1953**, *66*, 1187. (b) Waldron, R. D.; Badger, R. M. *J. Chem. Phys.* **1950**, *18*, 566. (c) Worsham, J. E.; Levy, H. A.; Peterson, S. W. *Acta Cryst.* **1957**, *10*, 319. (d) Sklar, N.; Senko, M. E.; Post, B. *Acta Cryst.* **1961**, *14*, 716. (e) Swaminathan, S.; Craven, B. M.; McMullan, R. K. *Acta Cryst.* **1984**, *B40*, 301.

(56) (a) Derreumaux, P.; Vergoten, G.; Lagant, P. *J. Comput. Chem.* **1990**, *11*, 560. (b) Saito, Y.; Machida, K.; Uno, T. *Spectrochim. Acta* **1971**, *A27*, 991.

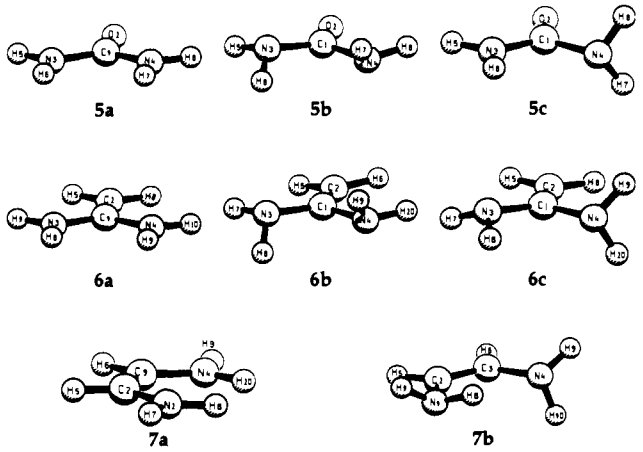

Figure 7. Optimized geometries for different conformations of compounds **5**, **6**, and **7**.

Table VIII. Calculated Bending Angle C–N–D (deg), Barrier of Rotation around C–NH_2 ΔE_{rot}(kcal/mol), and Barrier for Planarization ΔE_{plan} (kcal/mol) at MP2/6-31G(d) for **6b**, **1b**, and **5b**

	$(NH_2)_2CX$		
	6b X = CH_2	**1b** X = NH	**5b** X = O
C–N–D[a]	130.6	130.7 134.5	137.9
ΔE_{rot}	6.1	6.9	8.1
ΔE_{plan}	9.2	5.7	2.6

[a] See Table I.

value for the rotational barrier is only 7.4 kcal/mol (MP2/6-31G(d) + ZPE, Table V), calculated from the energy difference between **5b** and the transition state for rotation around the C–NH_2 bond **5c** (7.6 kcal/mol at MP4/6-311G(d,p), Table III). Also, the experimentally observed[55e] C–O bond for urea in the solid state at 12 K is significantly longer (1.265 Å) and the C–N bond is shorter (1.349 Å) than calculated here. The infrared spectrum of urea thin films on metal surfaces clearly indicates that **5** is distorted from the planar structure.[57] This may, however, be caused by the interactions of **5** with the metal surface.

The amino groups in **5b** are less pyramidalized than in **1b**, and the energy difference between the planar form and the equilibrium structure is smaller for **5** (2.6 kcal/mol) than for **1** (5, 7 kcal/mol, Tables I and V). This may be explained by the substitution of the NH group in **1** by the more electronegative and less π-donating oxygen in **5**, which induces a higher positive charge at carbon atom and stronger π-donation by the NH_2 groups in **5b** than in **1b**. Consequently, the barrier for rotation of one amino group in urea is *higher* than in guanidine. The energy difference between **5b** and **5c** is 8.1 kcal/mol, but only 6.9 kcal/mol between **1b** and **1c**.

The planar form of 1,1-diaminoethylene (**6a**) has three imaginary frequencies (Table VI). The equilibrium structure **6b** has two pyramidalized amino groups (bending angle 130.6°) and a planar CH_2 group, which is rotated by ~9° out of the heavy-atom plane (Figure 7). **6b** is predicted as 9.2 kcal/mol lower in energy than **6a** (9.8 kcal/mol at MP4/6-311G(d,p) Table III). This is reduced to 7.8 kcal/mol when corrections are made for ZPE contributions. Thus, **6** has clearly a nonplanar equilibrium geometry. Higher pyramidalization means lower barrier for rotation. The barrier for rotation of one NH_2 group in **6b** is only 6.1 kcal/mol (Table VI), lower than in **5b** (8.1 kcal/mol, Table V), because the oxygen atom in **5** is substituted by the less electronegative and stronger π-donating CH_2 group. The covalent bond order P(C–NH_2) increases in the order **5b** (0.936) < **1b** (0.940,0.954) < **6b** (0.968), reflecting the change in the polarity. Table VIII summarizes the results for molecules $(NH_2)_2CX$ (X = CH_2 (**6b**); X = NH (**1b**), X = 0 (**5b**)). The data clearly demonstrate that with increasing electronegativity of X there is (i) a higher barrier for rotation around the C–NH_2 group, (ii) a lower barrier for planarization of the NH_2 groups, and (iii) less pyramidalization of the amino groups.

(57) Suetaka, W. *Bull. Chem. Soc. Jpn.* **1967**, *40*, 2077.

Table IX. Calculated Topological Data for the Wave Functions of **5b** and **5c**[a]

	5b				**5c**			
	ρ_b	H_b	r_b	ϵ_b	ρ_b	H_b	r_b	ϵ_b
C^1–O^2	0.402	–0.700	0.331	0.137	0.400	–0.694	0.331	0.148
C^1–N^3	0.313	–0.464	0.374	0.131	0.326	–0.539	0.346	0.172
C^1–N^4	0.313	–0.464	0.374	0.131	0.286	–0.327	0.419	0.019
N^3–H^5	0.324	–0.453	0.759	0.039	0.325	–0.454	0.761	0.040
N^3–H^6	0.324	–0.451	0.754	0.041	0.326	–0.456	0.764	0.041
N^4–H^7	0.324	–0.451	0.754	0.041	0.320	–0.444	0.749	0.031
N^4–H^8	0.324	–0.453	0.759	0.039	0.320	–0.444	0.749	0.031

[a] For details see Table II.

Table X. Calculated Topological Data for the Wave Function of **6b** and **6c**[a]

	6b				**6c**			
	ρ_b	H_b	r_b	ϵ_b	ρ_b	H_b	r_b	ϵ_b
C^1–C^2	0.334	–0.394	0.543	0.517	0.336	–0.391	0.535	0.504
C^1–N^3	0.301	–0.425	0.379	0.114	0.305	–0.455	0.368	0.151
C^1–N^4	0.301	–0.425	0.379	0.114	0.284	–0.341	0.406	0.019
C^2–H^5	0.271	–0.276	0.641	0.043	0.271	–0.276	0.641	0.035
C^2–H^6	0.271	–0.276	0.641	0.043	0.272	–0.279	0.642	0.040
N^3–H^7	0.325	–0.453	0.751	0.039	0.325	–0.453	0.751	0.042
N^3–H^8	0.323	–0.449	0.751	0.040	0.325	–0.454	0.756	0.043
N^4–H^9	0.323	–0.449	0.751	0.040	0.323	–0.450	0.749	0.038
N^4–H^{10}	0.325	–0.453	0.751	0.039	0.322	–0.448	0.747	0.039

[a] For details see Table II.

The Laplacian distributions for **5b** and **6b** are shown in Figures 8 and 9; the results of the topological analysis of the wave function are listed in Tables IX an X. It is illuminating to compare the change in the electronic structure of the $(NH_2)_2C$–X bond for X = CH_2 (**6b**, Figure 9c) with X = NH (**1b**, Figure 4b) and X = 0 (**5b**, Figure 8c). The π-bond is polarized away from carbon toward X with increasing electronegativity of X. The bond critical point r_b for the C–X bond is much closer to C than to X for **1b** and **5b** (C–r_b/C–X < 0.5), but for **6b** it is closer to the terminal group (C–r_b/C–C > 0.5; Tables II, IX, and X). This means that the C–CH_2 bond in **6b** is polarized toward the central carbon atom and not toward the terminal carbon atom. Nevertheless, the central carbon atom carries a positive charge and the terminal C has a negative partial charge in **6b** (Table VI). The calculated ellipticity for the C–CH_2 in **6b** is very high (ϵ_b = 0.517), even higher than in ethylene (ϵ_b = 0.399). The ϵ_b value for the C–NH bond in **1b** is much lower (ϵ_b = 0.345), and it is also very low for the C–O bond in **5b** (ϵ_b = 0.137). This could be interpreted as an indication of a very low π-contribution to the C–O bond in urea. However, the bond critical poin' r_b in **5b** is very close to the carbon atom, while the π-bond is strongly polarized toward oxygen (Figure VIII).

1,1-Diaminoethylene (**6**) may be compared with the structural isomer *cis*-1,2-diaminoethylene (**7**). The planar form **7a** has three imaginary frequencies (Table VII). The equilibrium structure **7b** has two strongly pyramidalized amino groups. The lone-pair orbital of one NH_2 group is in conjugation with the C–C double bond, but the other amino group is rotated such that the lone-pair orbital is orthogonal to the C–C double bond (Figure 7). Structure **7b** is 9.8 kcal/mol more stable than **7a** (7.5 kcal/mol with ZPE correction). The cis isomer **7b** is 6.5 kcal/mol higher in energy than the geminal isomer **6b** (6.6 kcal/mol with ZPE correction).

The higher stability of geminal- over vicinal-substituted ethylenes has been the subject of numerous theoretical studies.[58,59] In many cases, π-conjugation has been used to explain the energy

(58) (a) Bernardi, F.; Bottoni, A.; Epiotis, N. D. *Theor. Chim. Acta* **1979**, *53*, 269. (b) Schleyer, P. v. R.; Kos, A. *Tetrahedron*, **1983**, *39*, 1141. (c) Frenking, G.; Koch, W.; Schaale, M. *J. Comput. Chem.* **1985**, *6*, 189.

(59) (a) Epiotis, N. D. *J. Am. Chem. Soc.* **1974**, *95*, 3087. (b) Epiotis, N. D. *Lecture Notes in Chemistry*; Springer: Berlin, 1983; p 257f. (c) Kollman, P. *J. Am. Chem. Soc.* **1974**, *96*, 4363.

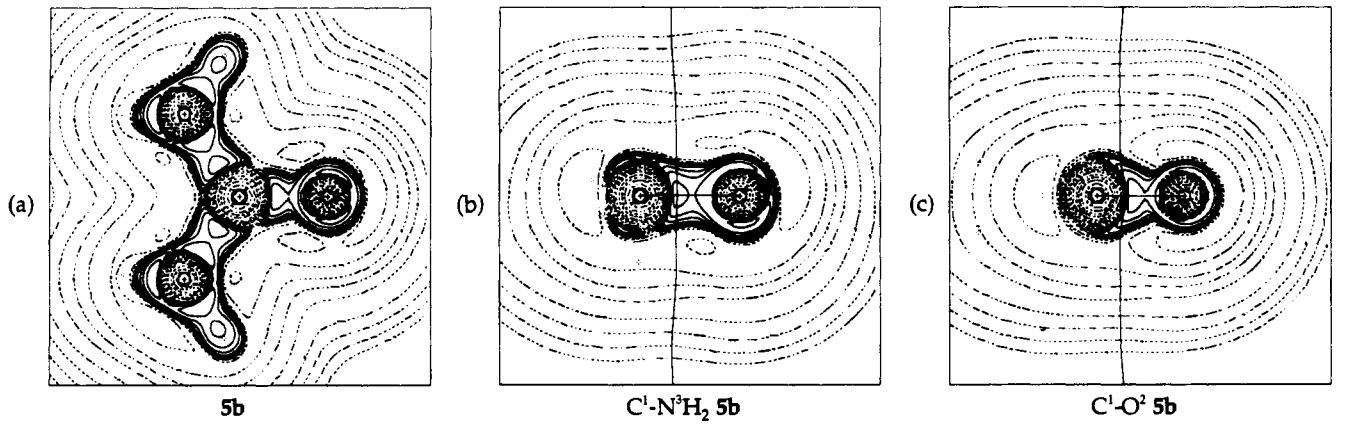

Figure 8. Contour line diagrams of the calculated Laplace distribution $-\nabla^2\rho(r)$ of the equilibrium geometry of urea (**5b**): (a) in the plane of the C and N atoms; (b) in the plane containing the $C^1-N^2H_2$ bond bisecting the NH_2 plane; (c) in the plane containing the C–O bond, perpendicular to the CN_2 plane. For details see Figure 4.

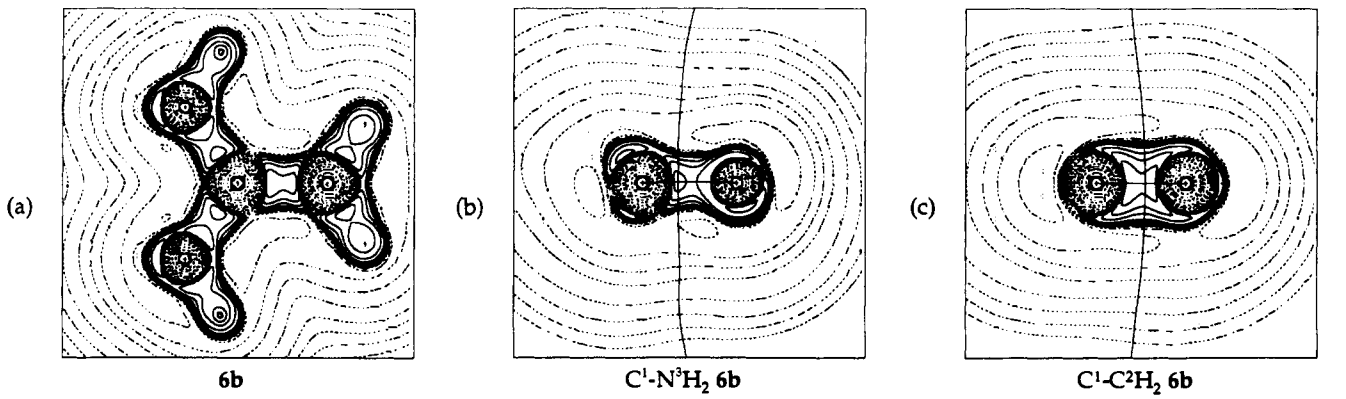

Figure 9. Contour line diagrams of the calculated Laplace concentration $-\nabla^2\rho(r)$ for the equilibrium geometry of 1,1-diaminoethylene (**6b**): (a) in the plane of the C and N atoms; (b) in the plane containing the $C^1-N^2H_2$ bond bisecting the NH_2 plane; (c) in the plane containing the $C^1-C^2H_2$ bond, perpendicular to the CN_2 plane. For details see Figure 4.

difference between the structural isomers.[58] It is useful to discuss the electronic structures of **6** and **7** by using the analogy to the allyl anion structure. Compounds **6** and **7** may be considered as 2-substituted and 1-substituted allyl anion systems. Figure 5 shows the MO diagram for the π-orbitals of the two systems. Substitution in the 2-position yields a stabilization of 0.318 β, while substitution in the 1-position gives only 0.204 β for the resonance stabilization. Thus, **7** is even less stabilized by conjugation than **6**. The orthogonal orientation of one amino group in **7** is stabilized by the formation of a hydrogen bond in **7b**, which makes the orthogonal form a minimum on the potential energy hypersurface. Two factors favor **6b** over **7b**. One reason is the slightly higher conjugative stabilization (0.318 β versus 0.204 β). This seems to be the main reason for the lower energy of **6b**, because the energy difference between **6** and **7** becomes nearly zero when one amino group in **6b** is rotated; **6c** is only 0.4 kcal/mol lower in energy than **7b** (Tables VI and VII). Thus, the conformation of **6** is important for its stability relative to **7**. The Y-conjugated form is additionally stabilized by the more favorable charge distribution in **6b**. Both methods of population analysis assign strong positive charges to the central carbon atom in **6b**, and strong negative charges to the atoms bound to it (Tables VI and VII).

4. Summary

The equilibrium geometries of the Y-conjugated compounds guanidine (**1**), guanidinium cation (**2**), urea (**5**), and 1,1-diaminoethylene (**6**) are theoretically predicted to be nonplanar. The energy minimum geometry of **1b** has strongly pyramidal amino groups. Structure **1b** is 6.7 kcal/mol lower in energy than the planar form **1a**. The energy minimum conformation of the guanidinium cation **2b** has planar amino groups which are rotated by ~15° out of planarity. Structure **2b** is little (<1 kcal/mol) lower in energy than the planar form **2a**. With inclusion of zero-point energy corrections, **2a** becomes even more stable than **2b**. The energy minimum conformations **5b** and **6b** have also pyramidal amino groups. The pyramidalization of the NH_2 groups and the rotation around the $C-NH_2$ bond increase for $(NH_2)_2CX$ compounds with increasing electronegativity of X, i.e., **6b** < **1b** < **5b**. The resonance stabilization of the Y-conjugated structures is not very high, because the rotation of one amino group leaves a subunit which is isoelectronic to the allyl anion. But the importance of resonance stabilization in the Y-shaped compounds **1**, **2**, **5**, and **6** is demonstrated by the calculated rotational barriers and lengthening of the $C-NH_2$ bonds upon rotation. The stabilization of the Y-shaped compounds relative to linear structures appears to be mainly due to the conjugative stabilization. This becomes obvious by the calculated relative energies of 1,1-diaminoethylene (**6**) and 1,2-diaminoethylene (**7**). The two isomers have nearly the same energy when one amino group in **6** is rotated, thus eliminating the conjugation of the lone-pair electrons. The very high basicity of guanidine, however, is not caused by the conjugative stabilization of **2**. The calculated proton affinity of **1** is similar to the proton affinity of *n*-Bu_3N, which has a basicity three orders of magnitude lower than **1**. The high basicity of **1** must be caused by other reasons such as strong hydrogen bonding of **2** in solution.

Acknowledgment. We thank Professor Josef Klein for stimulating discussions. Financial support by the Deutsche Forschungsgemeinschaft and the Fonds der Chemischen Industrie is gratefully acknowledged. Further support was provided by the computer companies Convex and Silicon Graphics. Additional computer time was given by the HLRZ Jülich and the HHLR Darmstadt.